State and Parameter Estimation of Triangular Layered Networks with Saturated Interconnections

Adel M. Annabi, Jean-Baptiste Pomet, Dario Prandi, and Ludovic Sacchelli

***Abstract*—We study the online state and parameter estimation of a p-layer triangular network where the interconnections are saturating nonlinearities. All coupling matrices and bias terms are unknown, and each linear part is known up to a bounded perturbation of a nominal Hurwitz matrix. Only the first layer is measured, and every layer is controlled. In this model the unknown parameters enter the dynamics multiplied by the saturation of states that are not measured, so the estimation involves a product of two unknown terms. We propose a protocol that exploits the nature of the saturation function to lift this ambiguity. The control inputs steer the saturation outputs through prescribed values, isolating one block of unknowns at a time and keeping every entry of the regressor known. All couplings and biases are then recovered exactly, in finite time and at instants computable in advance. The procedure is inherently online, since each stage constructs its inputs from the estimates delivered by the previous one. Numerical simulations illustrate the method.**

***Index Terms*—Parameter identification, experiment design, saturated systems, block-oriented systems, sliding-mode differentiators, networked systems.**

I. Introduction

This paper studies the identification of layered networks whose interconnections pass through a known saturation. Each layer obeys linear dynamics driven by the outputs of the other layers, each passed through a known sigmoid applied componentwise; the coupling matrices and biases are unknown, and so are the linear parts, up to a nominal Hurwitz term within a bounded perturbation. In system identification, cascades of static nonlinearities and linear blocks (Hammerstein–Wiener structures and their multi-layer extensions) have long offered models of this shape [1], [2], and there the design of the excitation is recognized as central, whether for open-loop or closed-loop experiments [3], [4], [5]. We take this point of view further. In the present class the saturation itself lets one prescribe the values that the regressor will visit, so persistency of excitation stops being a hypothesis on the data and becomes part of the construction.

A prominent instance comes from neuroscience. In the Wilson–Cowan equations [6], coupled neural populations interact through saturating firing rates, and layered variants remain standard tools for macroscopic cortical dynamics [7], [8]. Their parameters are poorly identified [9], [10], [11], and gains such as synaptic couplings drift over time [12], which motivates estimators that adapt online [13].

When the state is only partially measured, adaptive observers are the natural tool [14], and they have been built for several population models: conductance-based [15], delayed neural fields [16], [17] related to [18], [19], and Jansen–Rit [20], [21]. Their convergence typically requires dissipativity, persistency of excitation along the trajectory visited, or strong structural assumptions on the system. How much richness a given law needs is itself an active object of study [22], [23], [24], [25]. These works analyze or optimize a given source of excitation; none can create one where the trajectory carries none. That is precisely what the saturation allows here.

Our approach is to design the experimental inputs explicitly so as to force identifiability at each stage. By steering the saturation outputs through prescribed values we lift the ambiguity that saturations otherwise create, and we retrieve the parameters with an exact differentiator and least-squares fits. The estimation is necessarily online and recursive, since each stage uses the estimates of the previous one to construct its inputs. The main result is that all unknown parameters of a general network with an arbitrary number of layers are recovered exactly in finite time.

The protocol is described in Section III; the statements are Theorems 4 and 5. They differ on one parameter, namely the linear part of a layer that is not measured. The first theorem takes it as known; the second identifies it when the layer admits persistently exciting band references (Assumption 7), and Proposition 6 shows that this condition is necessary.

A preliminary version of these results appeared in [26], where the interconnection matrices of a layered network are identified under the assumptions that the linear part of every layer is known and equal to minus the identity, that the biases vanish, and that the inputs act through the identity. The present paper removes these restrictions: the linear parts are unknown up to a known nominal Hurwitz part (and identified under Assumption 7 below), the biases are unknown, the input matrices are arbitrary invertible ones, and the existence statements of [26] are replaced by the explicit protocol of Section III, with closed-form estimators and an explicit identification time. The protocol below rests on four auxiliary results, developed for a single saturated layer: regression on prescribed saturation patterns, steering of an unmeasured state into saturation, chaining of such steers, and output-feedback

Adel M. Annabi, Jean-Baptiste Pomet, and Ludovic Sacchelli are with Université Côte d'Azur, Inria, CNRS, LJAD, France (email: adel-malik.annabi@inria.fr, jean-baptiste.pomet@inria.fr, ludovic.sacchelli@inria.fr).

Dario Prandi is with Université Paris-Saclay, CNRS, CentraleSupélec, Laboratoire des Signaux et Systèmes, 91190, Gif-sur-Yvette, France (email: dario.prandi@centralesupelec.fr).

This work has been partially supported by the ANR-20-CE48-0003.

tracking inside the band. They are stated in Section IV.

The paper is organized as follows. Section II defines the model, the assumptions and the notion of protocol. Section III presents the protocol and the two identification theorems. Section IV states the auxiliary results used in their proofs. Section V collects the design results on which the realization of the protocol rests. Section VI reports simulations, Section VII the limitations. The proofs of the main theorems are in the appendix.

II. Problem statement

Notation: For integers $m < n$, $[\![m, n]\!] := \{i \in \mathbb{Z} : \ m \le i \le n\}$. $\mathbf{1}_d \in \mathbb{R}^d$ has all entries equal to 1, and $e_1, \dots, e_d$ is the canonical basis of $\mathbb{R}^d$. Given $g : \mathbb{R} \to \mathbb{R}$ and $z \in \mathbb{R}^d$, $g(z) := (g(z_1), \dots, g(z_d))^\top$. For $L > 0$ and $X \subset \mathbb{R}^d$, $C^{1,L}(\mathbb{R}, X)$ is the set of C^1 curves with values in X whose derivative is bounded by L. $\|\cdot\|$ is the Euclidean norm, $\|\cdot\|_\infty$ the max norm. For $M_1 \in \mathbb{R}^{d\times d_1}$, $M_2 \in \mathbb{R}^{d\times d_2}$ and $v \in \mathbb{R}^d$, $[M_1 \mid M_2 \mid v] \in \mathbb{R}^{d\times(d_1+d_2+1)}$ is the horizontal concatenation. $\lceil\sigma\rfloor^a := |\sigma|^a \operatorname{sign}(\sigma)$, with sign the set-valued sign, so that $\lceil\sigma\rfloor^{1/2} = \operatorname{sign}(\sigma)\sqrt{|\sigma|}$. Bounds that mix the Euclidean and the max norm absorb the conversion factor $\sqrt{d}$.

A. The model

We consider a network of p layers,

$$\begin{cases} \dot V_k = A_k V_k + \displaystyle\sum_{j=1}^{\min(k+1,p)} W_{kj} S(V_j) + B_k u_k + h_k, \\ y = V_1, \end{cases} \tag{1}$$

for $k \in [\![1, p]\!]$, where $V_k \in \mathbb{R}^{n_k}$ is the state of the k-th layer, $u_k \in \mathbb{R}^{n_k}$ its control, and only the first layer is measured. We write $n_1 \ge n_2 \ge \cdots \ge n_p$ and $V := (V_1, \dots, V_p)$. The parameters of (1) are collected, layer by layer, in

$$\Theta_k := \Big((A_i, h_i)_{i\le k},\ (W_{ij})_{i\le k,\ j\le \min(i+1,p)} \Big), \tag{2}$$

and $\Theta := \Theta_p$. Thus Θ_k gathers the first k rows of the network, including the coupling $W_{k,k+1}$ to the first unidentified layer.

The structure is feedforward with one step of overlap. Layer k receives $S(V_j)$ from every layer $j \le k$ and from the next layer through $W_{k,k+1}$ alone. The word *triangular* refers to this zero pattern of the block matrix $(W_{kj})_{k,j}$.

B. Assumptions

Assumption 1 (Linear part, known nominally)**.** For each $k \in [\![1, p]\!]$, $A_k = A_k^0 + \tilde A_k$ where $A_k^0 \in \mathbb{R}^{n_k\times n_k}$ is *known* and Hurwitz and $\|\tilde A_k\| \le \varepsilon_0$, for some $\varepsilon_0 > 0$ satisfying the explicit smallness condition (6) below; ε_0 is part of the known data.

Assumption 2 (Biases)**.** Each $h_k \in \mathbb{R}^{n_k}$ is unknown and $\|h_k\| \le \bar h$ for a known $\bar h > 0$.

Assumption 3 (Interconnections)**.** Each W_{kj} is unknown and $\|W_{kj}\| \le \bar W$ for a known $\bar W > 0$. In addition, $n_k \ge n_{k+1}$ and $\operatorname{rank} W_{k,k+1} = n_{k+1}$ for $k \in [\![1, p-1]\!]$, so that $W_{k,k+1}^\dagger := (W_{k,k+1}^\top W_{k,k+1})^{-1} W_{k,k+1}^\top$ satisfies $W_{k,k+1}^\dagger W_{k,k+1} = I_{n_{k+1}}$.

Assumption 4 (Saturation)**.** $S : \mathbb{R} \to [0, 1]$ is a known sigmoid, applied componentwise to vectors. It is globally Lipschitz, piecewise C^2 with bounded derivatives on each piece, satisfies

$$x \le \underline R \ \Rightarrow\ S(x) = 0, \qquad x \ge \bar R \ \Rightarrow\ S(x) = 1 \tag{3}$$

for known levels $\underline R < \bar R$, and is strictly increasing on $[\underline R, \bar R]$. We set $R := \max\{|\underline R|, |\bar R|\}$.

The inverse of S is defined on $(0, 1)$ only, and its Lipschitz constant blows up at the two saturation levels. Both the feedback law that keeps a layer in the band (Section V) and the descent of Section III use, instead, its truncation at a margin ω. For $\omega \in (0, 1/4)$ we write

$$S^\dagger(\sigma) := S^{-1}\big(\min\{\max\{\sigma, \omega\}, 1-\omega\}\big), \qquad \sigma \in \mathbb{R}, \tag{4}$$

extended componentwise, and

$$\begin{aligned} \Omega_\omega^d &:= \big[S^{-1}(\omega),\, S^{-1}(1-\omega)\big]^d, \\ L_\omega &:= \operatorname{Lip}\big(S^{-1}|_{[\omega,1-\omega]}\big) < \infty. \end{aligned} \tag{5}$$

Thus $S^\dagger$ is defined on all of $\mathbb{R}$, is globally L_ω-Lipschitz, takes its values in Ω_ω^1, and coincides with S^{-1} on $[\omega, 1-\omega]$; equivalently, $S^\dagger(S(x)) = x$ for every $x \in \Omega_\omega^1$.

Assumption 5 (Input matrices)**.** Each $B_k \in \mathbb{R}^{n_k\times n_k}$ is known and invertible.

Assumption 5 is the most demanding one experimentally, since it grants every layer, measured or not, a full-rank actuation channel with calibrated gain. If a deep layer carries no actuator, the protocol loses its hold on that layer. The descent of Section III can no longer place its state in Ω_ω, so $\hat V_j$ and every row below become unavailable, although part of row j may still be recoverable from the regressor built on its neighbours.

Assumptions 1–5 are in force throughout. Section III requires in addition exactly one of the two below, and the choice decides one question, namely whether the linear part of an unmeasured layer can be identified.

Assumption 6 (Known linear parts on the unmeasured layers)**.** $\tilde A_k = 0$ for every $k \in [\![2, p]\!]$; that is, $A_k = A_k^0$ is known for $k \ge 2$, while A_1 remains unknown.

Assumption 7 (Persistently exciting band references)**.** For every $k \in [\![2, p]\!]$ there exist references $\gamma_j \in C^{1,L}\big(\mathbb{R}, \Omega_{2\omega}^{n_j}\big)$, $j \in [\![1, k]\!]$, such that the reference regressor

$$\big(\gamma_k;\ 1;\ S(\gamma_1);\ \dots;\ S(\gamma_k)\big)$$

is persistently exciting, in the sense of Definition 14.

Remark 1 (Existence of band references)*.* Assumption 7 is a condition on the activation, not a structural one: such references exist as soon as S is not affine on the invertible region $\Omega_{2\omega}$. Indeed, if the components of $\psi := (\gamma_k;\ 1;\ S(\gamma_1); \dots; S(\gamma_k))$ are linearly independent on the box $\Omega_{2\omega}^{n_1} \times \cdots \times \Omega_{2\omega}^{n_k}$, a sinusoidal curve with rationally independent frequencies sweeps the box densely, and Weyl's equidistribution [27] makes the window Gramians of $\psi(\gamma)$ converge to a positive-definite average, so that the reference

regressor is persistently exciting. When S is affine on $\Omega_{2\omega}$, the block $S(\gamma_k)$ is an affine function of γ_k and no band reference of layer k can excite the full regressor; Proposition 6 shows that this is a genuine obstruction for band-confined experiments. Stage 1 needs no reference: its regressor is excited by the measured layer crossing the saturation levels.

A layer $k \geq 2$ is seen only through $S(V_k)$, hence only while V_k lies in the band. On an affine piece of that band, $A_k V_k$ cannot be told from $W_{kk} S(V_k)$, whatever the input (Proposition 6). Assumption 6 removes the question; Assumption 7 answers it. The measured layer is affected by neither, since V_1 is available saturated or not and S is affine on no interval containing a saturation level, so A_1 is identified in both regimes.

Throughout, $\rho > 0$ is a known bound on the initial condition, $\|V(0)\| \leq \rho$, and $M_k \geq 1$, $\alpha_k > 0$ are constants with $\|e^{A_k^0 t}\| \leq M_k e^{-\alpha_k t}$ for $t \geq 0$. The perturbation bound of Assumption 1 is required to satisfy

$$\varepsilon_0 \;\leq\; \min_{k \in [\![1,p]\!]} \frac{\alpha_k}{8 M_k \sqrt{n_k}}, \tag{6}$$

which involves only known data. Then $\varepsilon_0 < \min_k \alpha_k / M_k$, so that each A_k is Hurwitz too, with

$$\left\| e^{A_k t} \right\| \leq M_k e^{-\underline{\alpha}_k t}, \qquad \underline{\alpha}_k := \alpha_k - M_k \varepsilon_0 \geq \tfrac{7}{8} \alpha_k > 0. \tag{7}$$

Under a bounded input the network is then uniformly bounded, for every $\bar{W}$ and with an explicit absorbing radius; no small-gain or dissipativity condition is imposed anywhere in this paper. This is Proposition 16, stated in Section V where it is first used.

C. Protocol

All the controls and estimators below are constructed from the known data

$$\mathcal{D} := \big((A_k^0, B_k)_k,\, S,\, \underline{R},\, \bar{R},\, \bar{W},\, \bar{h},\, \varepsilon_0,\, \rho \big) \tag{8}$$

and from the measured output up to the current time, so that they never depend on the unknown parameters.

Definition 2 (Protocol)**.** A *protocol* is a pair of maps

$$u(t) = \mathcal{U}\big(t,\, y|_{[0,t]}\big), \qquad \hat{\Theta}(t) = \mathcal{F}\big(t,\, y|_{[0,t]}\big), \tag{9}$$

constructed from $\mathcal{D}$ alone. It *identifies* Θ *in time* T^* if $\hat{\Theta}(t) = \Theta$ for every $t \geq T^*$ and every solution of the closed loop (1)–(9) with $\|V(0)\| \leq \rho$.

Both maps in (9) are realized below by a finite-dimensional filter with a discontinuous right-hand side, so the closed loop is understood in the sense of Filippov; Remark 20 settles this point.

III. The protocol and the main results

A. The estimator

The protocol runs in p stages. Stage k occupies the interval $[T^{(k)}, T^{(k+1)}]$, is fed with the estimate $\hat{V}_k$ of the state of layer k, and returns the k-th row $\hat{\Theta}_k$ of the network together with an estimate $\hat{V}_{k+1}$ of the state of the next layer, which is the input of the following stage. Starting from $\hat{V}_1 := y$, this produces the chain

$$y = \hat{V}_1 \;\longrightarrow\; \hat{V}_2 \;\longrightarrow\; \cdots \;\longrightarrow\; \hat{V}_p, \tag{10}$$

along which the rows $\hat{\Theta}_1, \ldots, \hat{\Theta}_p$ are recovered sequentially (Figure 1). The unmeasured layers are never reconstructed by a dynamic observer. Each is obtained from the previous one by inverting the saturation, algebraically and at the current instant.

Stage k uses $1 + n_{k+1}$ time windows, with the convention $n_{p+1} := 0$. Throughout, we write

$$q_k := \min(k+1, p), \qquad N_k := \sum_{j=1}^{k} n_j. \tag{11}$$

The windows are one *regression window* $[r_k, r_k']$, on which the first k layers are held inside the invertible region Ω_ω along known references, and n_{k+1} *saturation windows*

$$\big[t_i^k,\; t_i^k + \tau + T\big], \qquad i \in [\![1, n_{k+1}]\!], \tag{12}$$

on which layer $k+1$, and it alone, is driven into saturation. They are pairwise disjoint subsets of $[T^{(k)}, T^{(k+1)}]$, and all of them, endpoints included, are fixed in advance and computable from the data $\mathcal{D}$ of (8). What the controls impose on the trajectory during each window is the content of Definition 15 in Section V; the estimator below uses nothing but their endpoints.

Layers $2, \ldots, k$ never leave Ω_ω, so their states are available through the chain (10) at every instant; layer 1 is measured and needs no such restriction. The values $S(V_j)$, $j \leq k$, are therefore computed rather than imposed. Only the state of layer $k+1$ is unavailable, and it is exactly the layer whose saturation the design prescribes.

Each stage k proceeds in three steps, of which (b) and (c) are empty when $k = p$. In step (a) (regression), the layers $j \leq k$ are steered along known references, so that $\|V_j - \gamma_j\|_\infty \leq \varepsilon$ on the regression window $[r_k, r_k']$, while layer $k+1$ is held at $S(V_{k+1}) = 0$; the row estimator (13d) returns the k-th row up to its forward coupling. In step (b) (forward coupling), layer $k+1$ is cycled through the saturation values $S(V_{k+1}) = e_i$, $i \in [\![1, n_{k+1}]\!]$, on the windows (12), with the layers $j \leq k$ kept inside Ω_ω; the estimator (13f) recovers $\hat{W}_{k,k+1}$. In step (c) (descent), layer $k+1$ is brought into $\Omega_\omega^{n_{k+1}}$, and the estimator (13g) returns $\hat{V}_{k+1} = V_{k+1}$ from the end of the descent on. Only layer $k+1$ is ever saturated, and the estimator and the design results of Section V are independent, as stated in Remark 8; the controls that realize (a)–(c) are built on the results of Section IV and the design results of Section V.

Fix a settling time $T > 0$; Proposition 18 provides gains (λ_1, λ_2) with $\lambda_2 > L_2$ and a gain L such that the differentiator is exact after time T. Its hypotheses hold along the protocol with computable constants, as shown at the end of Section V. Stage k of the protocol is, in its order of activation,

$$\begin{cases} \dot{\hat{z}}_{k,1} = B_k u_k + \hat{z}_{k,2} + \lambda_1 L \lceil \hat{V}_k - \hat{z}_{k,1} \rfloor^{1/2}, \\ \dot{\hat{z}}_{k,2} \in \lambda_2 L^2\, \operatorname{sign}\big(\hat{V}_k - \hat{z}_{k,1}\big), \end{cases} \tag{13a}$$

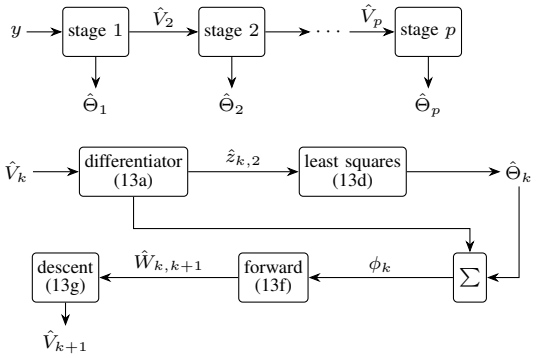

Figure 1. One stage of the estimator (stage k, repeated p times; last two blocks empty if $k = p$). The differentiator estimates the drift of layer k, the least-squares block the k-th row, the forward block the forward coupling, and the descent the next-layer state; the residual ϕ_k is formed at the $\sum$ node. Input $\hat{V}_k = y$ when $k = 1$; the stage returns $\hat{\Theta}_k$ and feeds $\hat{V}_{k+1}$ to the next stage, forming the chain $y = \hat{V}_1 \to \cdots \to \hat{V}_p$.

$$\Psi_k := \begin{bmatrix} \hat{V}_k \\ 1 \\ S(\hat{V}_1) \\ \vdots \\ S(\hat{V}_k) \end{bmatrix} \in \mathbb{R}^{\,n_k+1+N_k}, \tag{13b}$$

$$Z_k := \int_{r_k+T}^{r_k'} \hat{z}_{k,2}\, \Psi_k^\top \, dt, \qquad \Gamma_k := \int_{r_k+T}^{r_k'} \Psi_k \Psi_k^\top \, dt, \tag{13c}$$

$$\big[\hat{A}_k \mid \hat{h}_k \mid \hat{W}_{k1} \mid \cdots \mid \hat{W}_{kk}\big] := Z_k\, \Gamma_k^{-1}, \tag{13d}$$

$$\phi_k := \hat{z}_{k,2} - \hat{A}_k \hat{V}_k - \hat{h}_k - \sum_{j=1}^{k} \hat{W}_{kj} S(\hat{V}_j), \tag{13e}$$

$$\hat{W}_{k,k+1} := \frac{1}{\tau} \sum_{i=1}^{n_{k+1}} \int_{t_i^k+T}^{t_i^k+\tau+T} \phi_k \, e_i^\top \, dt, \tag{13f}$$

$$\hat{V}_{k+1} := S^\dagger\big(\hat{W}_{k,k+1}^\dagger \phi_k\big), \tag{13g}$$

initialized at $\hat{V}_1 := y$ and $\hat{z}_{k,\cdot}(0) := 0$, where the equations of (13a) are applied componentwise, $\hat{z}_{k,2}$ collects the second components, and $S^\dagger$ is the truncated inverse (4). Throughout, $\hat{W}_{k,k+1}^\dagger$ denotes the Moore–Penrose pseudoinverse, with the convention $0^\dagger = 0$; it coincides with the left inverse of Assumption 3 whenever $\hat{W}_{k,k+1}$ has full column rank, in particular once the estimate is exact. Equations (13e)–(13g) are omitted when $k = p$. The whole protocol is the concatenation of (13) for $k = 1, \ldots, p$, each stage being run with the estimates produced by the previous ones; $\hat{\Theta}$ is set to 0 on the entries not yet produced, and under Assumption 6 the known blocks $A_k = A_k^0$, $k \geq 2$, are copied verbatim, so that (15) holds in both regimes. Every right-hand side in (13) involves the output y, the earlier estimates and the known data $\mathcal{D}$ only, so (13) is a protocol in the sense of Definition 2. The steps (a)–(c) above list what is imposed on the trajectory during each window and which equation of (13) consumes it.

A single regression (13d) returns the whole k-th row of the network except its forward coupling, once the regressor is persistently exciting. It is legitimate because every entry of Ψ_k is known. The states $\hat{V}_j = V_j$, $j \leq k$, are supplied by the chain (10), and S is known. What the design must arrange is that Ψ_k be persistently exciting.

Under Assumption 6 the block $\hat{V}_k$ of Ψ_k carries no unknown at the stages $k \geq 2$, and is removed. One regresses $\hat{z}_{k,2} - A_k \hat{V}_k$ on

$$\Psi_k^\circ := \big[1;\ S(\hat{V}_1);\ \ldots;\ S(\hat{V}_k)\big] \in \mathbb{R}^{1+N_k} \tag{14}$$

and obtains $[\hat{h}_k \mid \hat{W}_{k1} \mid \cdots \mid \hat{W}_{kk}]$; the residual (13e) then reads with the true A_k in place of $\hat{A}_k$ at those stages. The reduced regressor is exciting under Assumption 4 alone, and so is Ψ_1, since the reference of the measured layer may cross the saturation levels, and S is affine on no interval containing a saturation level. At the stages $k \geq 2$ the full regressor is exciting under Assumption 7. Were S affine in the band, its block $S(\hat{V}_k)$ would be an affine function of its block $\hat{V}_k$ and Γ_k would be singular for every input; this is the content of Proposition 6 below.

Remark 3. The truncation in (13g) is what makes $\hat{V}_{k+1}$ defined at all times, since the untruncated S^{-1} is defined only on the invertible region, which is guaranteed only after step (c) has taken effect, so it would not define a protocol in the sense of Definition 2. By (4), $\hat{V}_{k+1} = V_{k+1}$ exactly as soon as $\hat{W}_{k,k+1} = W_{k,k+1}$ and $V_{k+1} \in \Omega_\omega^{n_{k+1}}$.

B. Exact identification

Theorem 4. *Let Assumptions 1–6 hold and let $\rho > 0$, and let* (13d) *be run with the reduced regressor* (14) *at the stages $k \geq 2$. Then there exists a protocol identifying Θ in an explicit time $T^* > 0$, constructed from $\mathcal{D}$ alone, such that every solution of the closed loop* (1)*,* (13) *with $\|V(0)\| \leq \rho$ satisfies*

$$\hat{\Theta}_k(t) = \Theta_k \quad \forall t \geq T^*, \qquad k \in [\![1, p]\!], \tag{15}$$

and

$$\hat{V}_{k+1}(t) = V_{k+1}(t) \quad \forall t \geq T^*, \qquad k \in [\![1, p-1]\!]. \tag{16}$$

The rows are delivered in order: there are instants $0 = T^{(1)} < \cdots < T^{(p+1)} = T^*$, computable in advance, such that $\hat{\Theta}_k = \Theta_k$ and $\hat{V}_{k+1} = V_{k+1}$ for every $t \geq T^{(k+1)}$.

Theorem 5. *The conclusion of Theorem 4 holds verbatim with Assumption 6 replaced by Assumption 7 and the reduced regressor by the full regressor* (13b) *at every stage $k \geq 2$ (stage* 1 *already uses the full regressor). In that regime no A_k is known, and*

$$\hat{A}_k(t) = A_k \quad \forall t \geq T^*, \qquad k \in [\![1, p]\!]. \tag{17}$$

Both proofs are in the appendix; they differ in one paragraph. The next proposition says that the alternative between the two assumptions is not an artifact of the protocol.

Proposition 6. *Let $k \in [\![2, p]\!]$ and suppose S is affine, with slope $s \neq 0$ and offset c_S, on a subinterval $I \subset (\underline{R}, \bar{R})$. Then for every $\mathcal{A} \in \mathbb{R}^{n_k \times n_k}$ the parameter sets (A_k, W_{kk}, h_k) and*

$$\big(A_k + \mathcal{A},\ W_{kk} - \mathcal{A}/s,\ h_k + (c_S/s)\,\mathcal{A}\mathbf{1}_{n_k}\big) \tag{18}$$

produce the same output along every solution of (1) *on which V_k takes its values in I^{n_k}. Every small enough $\mathcal{A}$ keeps the*

perturbed parameters within the bounds of Assumptions 2–3, so the two parameter sets are both admissible. Consequently no protocol confining layer k to I^{n_k} identifies A_k, and Assumption 7 cannot be dropped from Theorem 5.

Proof. Substitute (18) into the k-th line of (1) and use $S(x) = sx + c_S$ on I. The modified drift is

$$\begin{aligned}(A_k + \mathcal{A})V_k + \big(W_{kk} - \mathcal{A}/s\big)S(V_k) + h_k + (c_S/s)\mathcal{A}\mathbf{1}_{n_k} \\ = \; A_k V_k + W_{kk} S(V_k) + h_k,\end{aligned}$$

since the three added terms cancel on I^{n_k}. The two systems therefore share every solution as long as V_k stays in I^{n_k}, hence the same output, while the parameters differ by an arbitrary nonzero $\mathcal{A}$. No protocol confining layer k to that region separates them. □

Remark 7 (Observability decides). The dichotomy is between the region on which a layer is observable and the region on which S is curved. Layer $k \geq 2$ is observable only while it lies in the band, so its linear part needs persistently exciting band references. Layer 1 is observable on all of $\mathbb{R}$, and S is affine on no interval containing a saturation level, so A_1 is identified with no further assumption, and the protocol may drive V_1 across a saturation level to obtain the excitation, which is what [26] does for the couplings.

Remark 8 (Separation of design and estimation). The proof splits into two halves with disjoint hypotheses. The first shows that (13) returns the exact parameters along *any* bounded trajectory realizing the saturation pattern of steps (a)–(c), and uses only the saturation structure, Assumptions 3–4, and the differentiator; the second produces one such trajectory, and uses Assumptions 1–5 and none of the estimators. The estimator is therefore portable. The design of Section V may be replaced by any other means of imposing the pattern without touching (13).

Remark 9 (Recursive implementation). Run on the same signals, the batch estimators (13d) and (13f) coincide with recursive least-squares updates fed with the same data. The protocol is therefore implementable online with memory of order the square of the regressor dimension, and under zero noise each estimate is exact as soon as its running Gramian becomes invertible, no later than the end of the window.

IV. Auxiliary results

The protocol of Section III and the design of Section V rely on four auxiliary results: regression on a prescribed saturation pattern, steering of an unmeasured layer into prescribed saturation levels, chaining of such steers, and output-feedback tracking inside the band. They are stated here in the notation of the present paper; S is the componentwise sigmoid of Section II, so that the band constants below ($S^{-1}(\omega)$, L_ω) are computable from S. We admit the following results, which have been proven previously.

A. The auxiliary system

The results below concern one class of systems, of which every layer of (1) is an instance. Let $x \in \mathbb{R}^n$ solve

$$\begin{aligned}\dot{x} &= Ax + \phi(t) + Bu, \\ A &= A^0 + \tilde{A}, \quad \|\tilde{A}\| \leq \varepsilon_0, \quad \|\phi\|_\infty \leq \bar{\phi},\end{aligned} \tag{19}$$

with A^0 known Hurwitz, B known invertible and $\bar{\phi}$ known. Let $M \geq 1$ and $\alpha > 0$ satisfy $\|e^{A^0 t}\| \leq M e^{-\alpha t}$ for $t \geq 0$, and write $\underline{\alpha} := \alpha - M\varepsilon_0$, positive under (6). The k-th layer of (1) is of this form, with ϕ collecting the interconnection terms and the bias, so that one may take $\bar{\phi} = \bar{W}\sum_{j=1}^{q_k}\sqrt{n_j} + \bar{h}$, with q_k as in (11).

B. Regression on a prescribed saturation pattern

Given an *excitation design* $\mathcal{E} = \{(v_i, J_i)\}_{i \in [\![1,N]\!]}$, where the J_i are pairwise disjoint bounded intervals with $\tau_i := |J_i| > 0$, set

$$\begin{aligned}\Gamma(\mathcal{E}) &:= \sum_{i=1}^{N} \tau_i \, v_i v_i^\top, \\ E(z;\mathcal{E}) &:= \Big(\sum_{i=1}^{N} \int_{J_i} z(s)\, v_i^\top \, ds\Big)\Gamma(\mathcal{E})^{-1}.\end{aligned} \tag{20}$$

Lemma 10. *Let $\mathcal{E}$ be an excitation design with $\operatorname{rank}[v_1, \ldots, v_N] = n$ and let $z : [0,T] \to \mathbb{R}^q$ satisfy $z(t) = Wv_i$ for all $t \in J_i$ and all i. Then $\Gamma(\mathcal{E})$ is invertible and $E(z;\mathcal{E}) = W$. If instead $\operatorname{rank}[v_1, \ldots, v_N] = r < n$, then replacing $\Gamma(\mathcal{E})^{-1}$ by the Moore–Penrose pseudoinverse $\Gamma(\mathcal{E})^+$ returns $WP_{\mathcal{V}}$, where $\mathcal{V} = \operatorname{span}\{v_1, \ldots, v_N\}$.*

The estimator uses no knowledge of the dynamics and no state observer; identifiability comes from the saturation itself, the regressor $S(x(\cdot))$ being neither measured nor computable. A recursive least-squares implementation of the same regression is immediate.

C. Steering into the saturation levels

For a pattern $v \in \{0,1\}^n$, let K_v be the closed orthant of $\mathbb{R}^n$ carrying that pattern, trimmed at depth $R+1$:

$$K_v := \big\{x \in \mathbb{R}^n : \; (2v_i - 1)x_i \geq R + 1, \quad i \in [\![1, n]\!]\big\}, \tag{21}$$

and let $w_v \in \mathbb{R}^n$ be the vector with entries $(w_v)_i := R+1$ if $v_i = 1$ and $(w_v)_i := -(R+1)$ otherwise. By (3), $S(x) = v$ on K_v, since $R + 1 > \bar{R}$ and $-(R+1) < \underline{R}$. The vector w_v lies in the interior of K_v, at distance $R+1$ from its boundary, and its margin in K_v is

$$\delta_v := \frac{\operatorname{dist}(w_v, \mathbb{R}^n \setminus K_v)}{\|w_v\|} = \frac{1}{\sqrt{n}}. \tag{22}$$

Lemma 11 (Steering into a saturation level)**.** *Let $v \in \{0,1\}^n$ and $\rho, T_0 > 0$, set $\beta := (M/\alpha)\varepsilon_0$, $\beta_0 := \beta/(1-\beta)$ and $\hat{\delta}_v := (\delta_v - \beta_0)/(1+\beta_0)$, and suppose the smallness condition*

$$\beta \; < \; \frac{\delta_v}{1+\delta_v}, \qquad \textit{equivalently} \qquad \beta_0 \; < \; \delta_v, \tag{23}$$

which holds under (6) *for every pattern* v *and every* $n \geq 1$. *If* $T_0 > 2\alpha^{-1}\log(M/\hat{\delta}_v)$, *then for every* $\mu \geq \mu^\star$, *where*

$$\mu^\star := \max\left\{1,\ \frac{R+1+M\rho+2M\bar{\phi}/\alpha}{\big(\hat{\delta}_v - Me^{-\alpha T_0/2}\big)(1-\beta_0)\|w_v\|}\right\}, \quad (24)$$

the constant control

$$u \equiv -\mu\, B^{-1}A^0 w_v \quad (25)$$

makes every solution of (19) *with* $\|x(0)\| \leq \rho$ *satisfy*

$$S(x(t)) = v \quad \forall t \geq T_0, \qquad \|x(t)\| \leq R_\mu \quad \forall t \geq 0, \quad (26)$$

where $R_\mu := \mu(1+M)(1+\beta_0)\|w_v\| + M\rho + 2M\bar{\phi}/\alpha$.

Lemma 12. *Let* $\tau_{\mathrm{d}}, T_0 > 0$, *let* $t_1 < \cdots < t_N$ *satisfy* $t_{i+1} - (t_i + \tau_{\mathrm{d}}) > T_0$ *for* $i \in [\![1, N-1]\!]$ *and* $t_1 > T_0$, *and let* $v_1, \ldots, v_N \in \{0,1\}^n$. *Then there exists a piecewise constant control, computable from the known data, such that every solution of* (19) *with* $\|x(0)\| \leq \rho$ *satisfies*

$$S(x(t)) = v_i \qquad \forall t \in [t_i, t_i + \tau_{\mathrm{d}}], \quad \forall i \in [\![1, N]\!], \quad (27)$$

together with $\|x(t)\| \leq R_N$ *on* $[0, t_N + \tau_{\mathrm{d}}]$, *where* R_N *is obtained from the recursion* $\rho_1 := \rho$, $\rho_{i+1} := R_{\mu_i}$, *each* μ_i *being an amplitude supplied by Lemma 11 for the initial radius* ρ_i.

D. Tracking and state recovery

Lemma 13. *Consider* (19) *with* x *not measured and the signal* $\sigma(t) = S(x(t))$ *available. Let* $\omega \in (0, 1/4)$, *let* $\rho, \varepsilon, L > 0$, *let* $0 < T_1 < T_2$ *and let* $\gamma \in C^{1,L}(\mathbb{R}, \Omega^n_{2\omega})$. *Define, for* $\nu > 0$,

$$\eta_0(\sigma;\nu,\gamma,\omega) = \begin{cases} \nu, & \sigma \leq 0, \\ \ell_1(\sigma;\nu,\gamma), & 0 < \sigma < \omega, \\ -\nu\big(S^\dagger(\sigma) - \gamma\big), & \omega \leq \sigma \leq 1-\omega, \\ \ell_2(\sigma;\nu,\gamma), & 1-\omega < \sigma < 1, \\ -\nu, & \sigma \geq 1, \end{cases} \quad (28)$$

where ℓ_1 *and* ℓ_2 *are affine in* σ *and make* η_0 *continuous, and let* $\boldsymbol{\eta}_0$ *be its componentwise extension. The output feedback is*

$$u(t) = B^{-1}\boldsymbol{\eta}_0\big(\sigma(t);\nu,\gamma(t),\omega\big), \quad (29)$$

and there exists a threshold $\nu^\star > 0$, *computable from the known data, such that for every* $\nu > \nu^\star$ *every solution of the closed loop* (19), (29) *with* $\|x(0)\| \leq \rho$ *is defined on* $[0,\infty)$ *and satisfies*

$$x(t) \in \Omega^n_\omega \ \ \forall t \geq T_1, \qquad \|x(t) - \gamma(t)\|_\infty \leq \varepsilon \ \ \forall t \geq T_2. \quad (30)$$

The first assertion of the lemma keeps the state inside Ω_ω from the time T_1 on; there the state is recovered from the measured signal by inversion, $S^\dagger(S(x)) = x$ by (4), which is the state-recovery step of the protocol of Section III.

Both applications are direct. The results require the saturation to take fixed values on coradiant regions, met by a controllable direction; here the regions are the orthants (21) and, B being invertible, $\mathrm{Im}\big((A^0)^{-1}B\big) = \mathbb{R}^n$ meets every orthant interior. The tracking lemma requires only known linear-growth bounds on the drift, and the auxiliary system (19) satisfies $\|Ax + \phi(t)\| \leq (\|A^0\| + \varepsilon_0)\|x\| + \bar{\phi}$. Finally, the steering smallness condition (23) holds under (6): with $\beta \leq (M/\alpha)\varepsilon_0$ and $\varepsilon_0 \leq \alpha/(8M\sqrt{n})$ from (6), one has $\beta \leq 1/(8\sqrt{n}) < 1/(\sqrt{n}+1) = \delta_v/(1+\delta_v)$.

V. Excitation design

This section collects the design results that turn the results of Section IV into a schedule: the uniform bound of Proposition 16, the measured-state tracking of Lemma 17, and the differentiator of Proposition 18. The steering into saturation, the chaining of the saturation windows and the saturated tracking are Lemmas 11, 12 and 13 of Section IV.

A. The excitation schedule

Recall $q_k = \min(k+1, p)$ from (11).

Definition 14. A vector valued function $g \in C(\mathbb{R}, \mathbb{R}^q)$ verifies the *persistent excitation condition* (PE) if there exist $a, b, \tau > 0$ such that

$$a\, I_q \ \preccurlyeq\ \int_{t-\tau}^{t} g(s)g(s)^\top ds \ \preccurlyeq\ b\, I_q \quad (31)$$

for every t. If there exists $U \subset \mathbb{R}^q$ such that $g \in C(\mathbb{R}, U)$, we write $g \in \mathrm{PE}(U)$.

Definition 15 (Excitation schedule)**.** Let $\tau, T, T_0, T_{\mathrm{rel}}, L > 0$ and $\omega \in (0, 1/4)$, where T_{rel} is the relaxation time (35), computable from the known data, and let $\varepsilon > 0$ satisfy

$$\varepsilon \ <\ \min\big\{\, S^{-1}(2\omega) - S^{-1}(\omega),\ S^{-1}(1-\omega) - S^{-1}(1-2\omega)\,\big\}, \quad (32)$$

so that staying within ε of a reference in $\Omega_{2\omega}$ keeps the state inside Ω_ω. A *schedule* consists of times $0 = T^{(1)} < \cdots < T^{(p+1)}$, of windows as in (12) with $t^k_{i+1} - t^k_i \geq \tau + T + T_0 + T_{\mathrm{rel}}$, contained in $[T^{(k)} + T, T^{(k+1)}]$, of references $\gamma^{(k)}_1 \in C^{1,L}\big(\mathbb{R}, \mathbb{R}^{n_1}\big)$, bounded, whose crossings of the saturation levels are transversal (finitely many on each regression window, with $|\dot{\gamma}^{(k)}_{1,i}| \geq \tau_{\mathrm{tv}} > 0$ there) and confined to $\Omega^{n_1}_{2\omega}$ for $k \geq 2$, and of references $\gamma^{(k)}_j \in C^{1,L}\big(\mathbb{R}, \Omega^{n_j}_{2\omega}\big)$, $j \in [\![2, p]\!]$, such that every solution of the closed loop satisfies, for every $k \in [\![1, p]\!]$,

(S1) $V_j(t) \in \Omega^{n_j}_\omega$ for every $j \in [\![2, k]\!]$ and every $t \geq T^{(k)}$;
(S2) $\|V_j - \gamma_j\|_\infty \leq \varepsilon$ for every $j \in [\![1, k]\!]$, and $S(V_{k+1}) = 0$, on $[r_k, r'_k]$;
(S3) $S(V_{k+1}) = e_i$ on $[t^k_i,\, t^k_i + \tau + T]$, for every $i \in [\![1, n_{k+1}]\!]$;

and such that the reference regressor is persistently exciting; here the reference regressor is Ψ^γ_k under Assumption 7, and $\Psi^{\circ\gamma}_k$ under Assumption 6 and $k \geq 2$, where Ψ^γ_k and $\Psi^{\circ\gamma}_k$ are obtained from (13b) and (14) by replacing each $\hat{V}_j$ with $\gamma^{(k)}_j$. Every constant above is computable from the known data (8) alone.

Conditions (S1)–(S3) impose the trajectory constraints of steps (a)–(c). (S1) is the standing invariant of the protocol. Once a layer has been identified it is kept inside the region where the saturation is invertible, so that its state remains available through the chain (10). (S2) excites the identified layers along known references while switching off the contribution of layer $k+1$; (S3) switches that contribution back on, one coordinate at a time.

B. Saturation windows

Proposition 16. *Let Assumptions 1–4 hold and let u be measurable with $\|B_k u_k\| \le \bar{u}$ for every k. Then every solution of* (1) *with $\|V(0)\| \le \rho$ is defined on $[0,\infty)$ and satisfies*

$$\|V_k(t)\| \;\le\; M_k e^{-\underline{\alpha}_k t}\rho + R_\infty(\bar{u}), \qquad \forall t \ge 0, \tag{33}$$

for every $k \in [\![1,p]\!]$, where

$$R_\infty(\bar{u}) := \max_k \; \frac{M_k}{\underline{\alpha}_k}\Big(\bar{W}\sum_{j=1}^{q_k}\sqrt{n_j} \;+\; \bar{h} + \bar{u}\Big). \tag{34}$$

In particular the ball of radius $R_\infty(\bar{u})$ is absorbing, and $R_\infty(\bar{u})$ is computable from the known data.

Proof. Since $\|S(V_j(t))\| \le \sqrt{n_j}$, the k-th line of (1) is a linear equation driven by the bounded disturbance $\phi_k := \sum_j W_{kj}S(V_j) + h_k + B_k u_k$, whose norm obeys the bound of (34). Variation of constants with (7) gives (33) on the maximal interval of existence; since its right side stays finite on every finite interval, no finite escape time exists and solutions are global. □

The saturation windows themselves are realized by Lemmas 11 and 12 of Section IV, with the values $v = e_i$, $i \in [\![1, n_{k+1}]\!]$.

Between two saturation windows the control of layer $k+1$ vanishes, and by Proposition 16 the state returns to within $2R_\infty(0)$, the radius (34) evaluated with $\bar{u} = 0$, within a relaxation interval of length

$$T_{\mathrm{rel}} := \frac{1}{\underline{\alpha}_{k+1}} \log \frac{M_{k+1}R_\mu}{R_\infty(0)}, \tag{35}$$

where R_μ is the state bound of Lemma 11 for a single steering from the ball of radius $2R_\infty(0)$. One single amplitude μ therefore serves every window, and the state obeys a bound R_μ independent of the number of windows.

C. Tracking

Two tracking results are needed, and they differ in what is measured. The first uses the state itself and applies to the measured layer; it is stated here with its proof. The second operates on a layer whose state is not measured and of which only the saturation is observed; it is Lemma 13 of Section IV, and it is the one that puts (S1) in force and keeps it there.

Lemma 17. *Consider* (19) *with x available, let $\varepsilon, L, \rho, T_1 > 0$ and let $\gamma \in C^{1,L}(\mathbb{R},\mathbb{R}^n)$ be bounded. There exists $\mu_{\mathrm{tr}}^\star > 0$, depending only on $(A^0, \varepsilon_0, \|B^{-1}\|, \bar{\phi}, \|\gamma\|_\infty, \rho, T_1, \varepsilon)$, such that for every $\mu_{\mathrm{tr}} \ge \mu_{\mathrm{tr}}^\star$ the state feedback*

$$u = B^{-1}\big(-\mu_{\mathrm{tr}}(x-\gamma) + \dot{\gamma} - A^0 x\big) \tag{36}$$

yields, for every solution with $\|x(0)\| \le \rho$,

$$\|x(t) - \gamma(t)\|_\infty \le \varepsilon \qquad \forall t \ge T_1. \tag{37}$$

Proof of Lemma 17. With $e := x - \gamma$, the control (36) cancels the feedforward $\dot{\gamma}$ and closes the loop as $\dot{e} = -\mu_{\mathrm{tr}} e + \tilde{A}e + \tilde{A}\gamma + \phi$, so that, by Grönwall and $\|\tilde{A}\| \le \varepsilon_0$,

$$\|e(t)\| \le e^{-(\mu_{\mathrm{tr}}-\varepsilon_0)t}\big(\rho + \|\gamma\|_\infty\big) + \frac{\varepsilon_0\|\gamma\|_\infty + \bar{\phi}}{\mu_{\mathrm{tr}} - \varepsilon_0}.$$

Both terms are made $\le \varepsilon/2$ for every $t \ge T_1$ by any $\mu_{\mathrm{tr}} \ge \mu_{\mathrm{tr}}^\star$ with $\mu_{\mathrm{tr}}^\star$ computable from the listed data, and $\|e\|_\infty \le \|e\|$. □

Lemma 13 of Section IV applies to a layer whose saturation is measured and whose state is not: its hypotheses are met with the known linear-growth bound $\|Ax + \phi(t)\| \le (\|A^0\| + \varepsilon_0)\|x\| + \bar{\phi}$ of the auxiliary system, and its gain threshold $\nu^\star$ is computable from the known data, the gain ν being chosen above it.

D. Differentiation

The protocol switches its control at finitely many instants and differentiates a signal across those switches. The differentiator of [28] performs this exactly, with a convergence time that is tunable at will. We use it in the following form, adapted from [29]. Consider

$$\dot{z}_1 = g_1(z_1,t) + z_2, \qquad \dot{z}_2 = g_2(z_1,z_2,t), \qquad y = z_1, \tag{38}$$

with g_1 continuous and piecewise C^1, and g_2 continuous and piecewise C^1 with $\|g_2\| \le L_2$ for a known $L_2 > 0$. The observer

$$\begin{cases} \dot{\hat{z}}_1 = g_1(y,t) + \hat{z}_2 + \lambda_1 L \lceil y - \hat{z}_1 \rfloor^{1/2}, \\ \dot{\hat{z}}_2 \in \lambda_2 L^2 \,\mathrm{sign}\big(y - \hat{z}_1\big), \end{cases} \tag{39}$$

with $\lceil\cdot\rfloor^{1/2}$ and sign as in the Notation paragraph, has the following property.

Proposition 18. *There exist (λ_1,λ_2) with $\lambda_2 > L_2$ such that, for every $T > 0$ and every $\rho > 0$, there exists $L^\star > 0$ such that for every $L \ge L^\star$, every solution of* (38)–(39) *with $\|\hat{z}(t_0) - z(t_0)\| \le \rho$ satisfies*

$$\hat{z}(t) = z(t) \qquad \forall t \ge t_0 + T. \tag{40}$$

Proof. Between two discontinuities of g_2 this is the homogeneous second-order sliding-mode observer of [28], [29] with the weight vector $(2,1,0)$. Its convergence time is bounded by a function of the gains and of the initial error, and by homogeneity it can be made arbitrarily small by increasing L; any prescribed settling time $T > 0$ is achieved by a large enough L, computable from the data [28]. □

Applied to (13a), the input of the differentiator is $\hat{V}_k$, and the known term $B_k u_k$ is injected, so that the estimated quantity is

$$g_{k,i} := \Big(A_k V_k + h_k + \sum_{j=1}^{\min(k+1,p)} W_{kj}S(V_j)\Big)_i, \tag{41}$$

which is continuous. Between control switches $\dot{g}_{k,i}$ is bounded by a computable constant L_2 (the states and the controls are uniformly bounded along the protocol, by Proposition 16 and the amplitude bounds of Lemmas 11, 12 and 13), and at the switches $\dot{g}_{k,i}$ jumps by at most a computable Δ. The input $\hat{V}_k$ itself jumps by at most $\bar{J} := S^{-1}(1-\omega) - S^{-1}(\omega)$ at the stage start $T^{(k)}$, since before it $\hat{V}_k$ is clamped at a boundary of Ω_ω: the truncated inverse (4) outputs either $S^{-1}(\omega)$ or $S^{-1}(1-\omega)$ there. A single settling time T and one pair (λ_1,λ_2) with $\lambda_2 > L_2$ therefore serve the whole protocol: the gain L is

chosen by Proposition 18 for the time T and a radius covering the initial observer error and the jump bounds $\max\{\Delta, \bar{J}\}$, all computable, and by Remark 19 the differentiator (13a) is exact on every integration window.

Remark 19 (Switching). The proposition concerns a trajectory without discontinuities; along the protocol the input of the differentiator and its derivative jump at the switch instants. A jump of the input by at most $\bar{J}$ resets the error of $\hat{z}_1$ to at most $\bar{J}$, and a jump of its derivative by at most Δ resets the error of $\hat{z}_2$ to at most Δ, so the observer error is at most $\max\{\Delta, \bar{J}\}$ after every jump. By the proposition, the same gain L, chosen for the settling time T and a radius covering $\max\{\Delta, \bar{J}\}$ and the initial observer error, reconverges the observer within T; it is therefore exact on every interval that starts a time T after the last jump, and the windows of Definition 15 all lie in such intervals.

Remark 20 (Well-posedness). The controls of Lemmas 11, 12, 17 and 13 are measurable and piecewise continuous, so the plant (1) admits global Carathéodory solutions, unique between consecutive switching instants. Each differentiator (13a) has a discontinuous right-hand side; its solutions are understood in the sense of Filippov [30], and they are unique and classical off the sliding surface. The descent map (13g) is defined and globally Lipschitz at all times, by (4). The closed loop of Definition 2 is therefore well posed.

VI. Numerical experiments

The protocol of Section III is run on a two-layer instance $p = 2$ with $n_1 = 3$ measured and $n_2 = 2$ unmeasured coordinates, the smallest network on which the three steps of the protocol all appear. The activation is a clipped logistic

$$S(x) = \frac{\Lambda\big(a\,x\big) - \Lambda(-a)}{\Lambda(a) - \Lambda(-a)}, \qquad x \in (-1, 1), \tag{42}$$

with $a = 5$ and $\Lambda(u) = (1 + \mathrm{e}^{-u})^{-1}$, extended constantly so that $S(-1) = 0$ and $S(1) = 1$; on $(-1, 1)$ it is smooth with strictly positive derivative. The linear parts are Hurwitz with spectrum in $[-3.0, -1.8]$, drawn once at random from the seed 7 of the generating script as perturbations of norm $3 \cdot 10^{-2}$ of Hurwitz nominal parts, so that Assumption 1 holds; the couplings and the biases are drawn once at random with the same seed in the ranges of the known data (8), with $\bar{W} = 0.8$ and $\bar{h} = 0.4$. The instance is in the regime of Theorem 4 under Assumption 6. The matrix A_1 is unknown and identified, while the linear part A_2 of the unmeasured layer is given to the protocol. The margin is $\omega = 0.04$, so a coordinate of an unmeasured layer is recoverable exactly when it lies in $[S^{-1}(0.04), S^{-1}(0.96)] \simeq [-0.61, 0.61]$.

The measurement is corrupted throughout the run. The output obeys

$$y = V_1 + d, \qquad \|d\|_\infty \le \bar{d}, \tag{43}$$

with $\bar{d} = 3 \cdot 10^{-4}$; the noise is a sum of 30 sinusoids with frequencies spread over $[15, 50]$ rad/s, random amplitudes bounded by $\bar{d}$, and random phases (seed 23). It is zero-mean, with correlation time far below the window lengths, and every excitation frequency lies below 13 rad/s. The closed loop (1)–(13) is integrated with a fixed-step RK4 scheme of step $3 \cdot 10^{-4}$ s; the sign functions of (13a) are smoothed at $\varepsilon_{\mathrm{sm}} = 10^{-4}$.

The schedule imposed on the unmeasured layer alternates saturated and invertible regimes. Up to $r_1' = 47.5$ the measured layer tracks a sum of three sinusoids at the incommensurate frequencies $\pi\sqrt{11}, \pi\sqrt{13}, \pi\sqrt{17}$ rad/s while V_2 is held at $S(V_2) = 0$ by the open-loop steering law, and the regression (13d) over the window $[r_1 + T, r_1'] = [3, 47.5]$ delivers $(\hat{A}_1, \hat{h}_1, \hat{W}_{11})$. The two saturation windows $[49, 55.5]$ and $[58.5, 65]$ drive $S(V_2)$ to e_1 and then to e_2, and (13f) returns $\hat{W}_{12}$ over the sub-windows $[t_i + T, t_i + \tau + T]$, namely $[49.5, 55.5]$ and $[59, 65]$, with $t_1 = 49$ and $t_2 = 58.5$. The descent takes place on $[t_2 + \tau + T, T^{(2)}] = [65, 80]$, at the end of which V_2 has entered Ω_ω; from then on the trajectory is driven along the band references with $\hat{V}_2 = V_2$ and remains in the band. The regression of the second row over $[r_2 + T, r_2'] = [82.5, 302]$ finally delivers $(\hat{h}_2, \hat{W}_{21}, \hat{W}_{22})$, and $T^* = T^{(3)} = 302$. Each of these instants is computable in advance from the known data, as Theorem 4 requires.

Figures 2 and 3 report the identification errors along the run.

Remark 21 (What the curves show). Nothing in the run is asymptotic. At each instant t of a window, the plotted value is the closed-form batch estimator (13d) or (13f) evaluated on the recorded prefix $[r_k + T, t]$; by Remark 9, it is also the iterate of a recursive implementation fed with the same data. Under zero noise, each curve would drop to zero as soon as its running Gramian becomes invertible and stay there. The gradual decay in Figures 2 and 3 is the averaging of the noise over the growing window, not a convergence transient, and the freeze at the delivery instants is (15) up to the noise floor.

The three blocks of the first row (Figure 2) drop from $O(1)$ to $3.0 \cdot 10^{-4}$, $5.0 \cdot 10^{-4}$ and $7.4 \cdot 10^{-4}$ within the regression window and freeze at these values for every $t \ge r_1'$. The noise enters the regression only through the differentiator, whose output is integrated over a window of length 44.5 s, so the first row is barely affected.

The reconstruction of V_2 (Figure 3, top) is where the noise floor appears. Its envelope falls below $4.2 \cdot 10^{-2}$ over the second regression window and reaches $1.5 \cdot 10^{-2}$ at the end of the run. The second-row regression is run on zero-phase-filtered signals with cutoff 5 rad/s, below the noise band and above the excitation frequencies $0.25\pi\sqrt{31}, 0.25\pi\sqrt{37} \approx 4.4, 4.8$ rad/s of the band references; it removes the out-of-band contribution of the differentiator without introducing any lag. The batch estimator is computed at r_2' on recorded data. The row is then delivered at $2.1 \cdot 10^{-2}$, $1.9 \cdot 10^{-2}$ and $6.2 \cdot 10^{-2}$ for $\hat{h}_2$, $\hat{W}_{21}$ and $\hat{W}_{22}$.

VII. Conclusion

The protocol turns a triangular saturated network into a sequence of well-posed regressions. Each stage imposes the saturation pattern that makes its regressor known, fits one row of unknowns, and descends to the next layer by inverting the saturation algebraically. Exactness holds at instants computable in advance from the known data, and the dichotomy

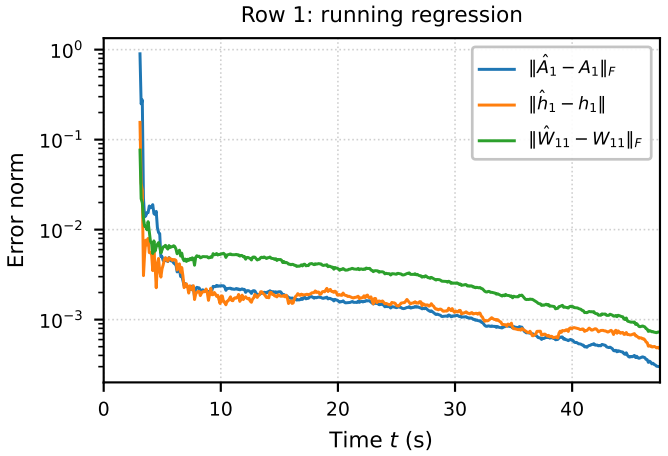

Figure 2. The first stage under the noise (43). The curves are running batch estimates, matrices in the Frobenius norm, vectors in the Euclidean norm, of the three blocks of the first row over the regression window $[r_1 + T, r_1'] = [3, 47.5]$.

of Section III says precisely when the linear part of an unmeasured layer can be recovered along with the rest.

The limitations are as follows. The nominal linear parts must be known within ε_0. Every layer must be actuated through a known invertible matrix; Section II discusses what this demands experimentally and what survives without it, and the steering amplitudes that drive unmeasured layers deep into saturation are part of the price of exactness. The forward couplings must be left-invertible; when $\operatorname{rank} W_{k,k+1} < n_{k+1}$ the descent cannot determine $S(V_{k+1})$ beyond the complement of its kernel, and no row below k is identified as a whole. One of Assumption 6 and Assumption 7 is needed, and Proposition 6 shows that the second cannot be weakened for band-confined, regression-based experiments; the saturated excursions of a layer do carry information on its linear part through flow-matching conditions rather than regressions, and exploiting them is open. The references of Assumption 7 exist as soon as the activation is not affine on the invertible region (Remark 1), and the identification time deteriorates continuously as the activation approaches an affine one. Discretization is not analyzed in this paper. The simulations of Section VI run a fixed-step scheme with smoothed sign injections, and their error floors reflect the smoothing and the descent, not a sampling analysis.

Appendix A
Proof of Theorem 4

For $k \in [\![1, p]\!]$ let $\mathcal{H}_k$ denote the property

$$\begin{aligned} \hat{\Theta}_{k-1} = \Theta_{k-1}, \quad \hat{V}_j(t) = V_j(t) \quad \forall t \geq T^{(j)}, \ \forall j \leq k, \\ V_j(t) \in \Omega_\omega^{n_j} \quad \forall t \geq T^{(j)}, \quad \forall j \in [\![2, k]\!]. \end{aligned} \tag{44}$$

$\mathcal{H}_1$ holds, since $\hat{V}_1 = y = V_1$, Θ_0 is empty, and no layer is yet confined. We prove $\mathcal{H}_k \Rightarrow \mathcal{H}_{k+1}$, which is (15). All windows of stage k are scheduled at least T after $T^{(k)}$, the time after which the stage-k differentiator is exact following the jump of its input.

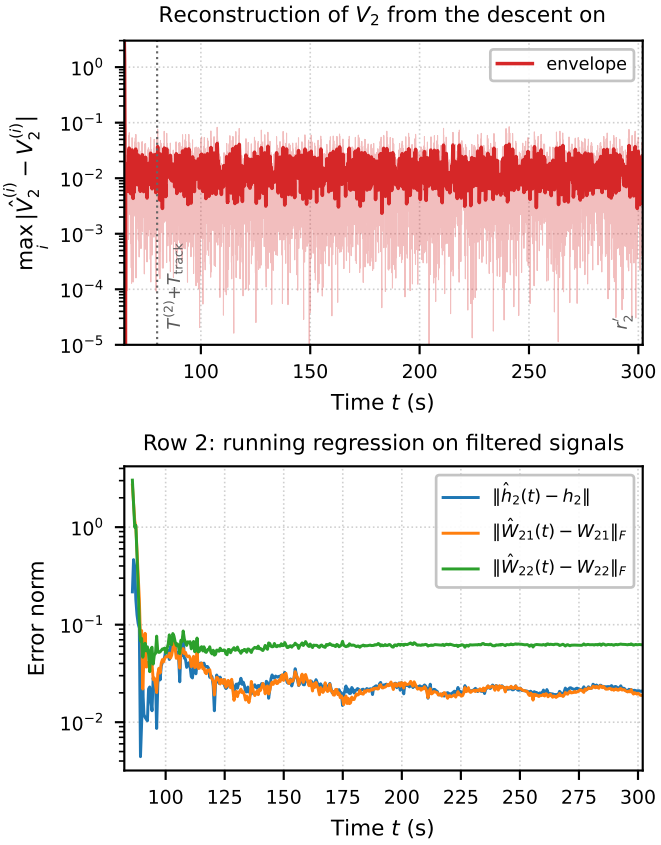

Figure 3. The second stage under the noise (43). Top: reconstruction error $\max_i |\hat{V}_2^{(i)} - V_2^{(i)}|$ from the descent on, raw trace light and envelope solid, on a logarithmic scale. The envelope is the raw trace passed through a zero-lag low-pass (second-order Butterworth, cutoff 3 rad/s, applied forward then backward) and is shown for readability only. Dotted lines mark the end of the descent (time 80) and the delivery $r_2' = 302$. Bottom: the three blocks of the second row over $[r_2 + T, r_2'] = [82.5, 302]$, computed on zero-phase-filtered signals with cutoff 5 rad/s.

Differentiation. By $\mathcal{H}_k$ the differentiator (13a) is driven by V_k itself, up to the jump of its input at $T^{(k)}$. Its sliding set is $\hat{z}_{k,1} = V_k$, $\hat{z}_{k,2} = \dot{V}_k - B_k u_k$, so that Proposition 18 gives, on each window of stage k,

$$\hat{z}_{k,2} = A_k V_k + h_k + \sum_{j=1}^{q_k} W_{kj} S(V_j). \tag{45}$$

The k-th row. On $[r_k + T, r_k']$, (S2) gives $S(V_{k+1}) = 0$, so that (45) reduces to

$$\hat{z}_{k,2} = \begin{bmatrix} A_k \mid h_k \mid W_{k1} \mid \cdots \mid W_{kk} \end{bmatrix} \Psi_k \tag{46}$$

under Assumption 7, and to

$$\hat{z}_{k,2} - A_k \hat{V}_k = \begin{bmatrix} h_k \mid W_{k1} \mid \cdots \mid W_{kk} \end{bmatrix} \Psi_k^\circ \tag{47}$$

under Assumption 6 and $k \geq 2$. This is the only place where the two regimes differ. In both, every entry of the regressor is the true one, since $\hat{V}_j = V_j$ for $j \leq k$ by $\mathcal{H}_k$; the reference regressor is persistently exciting by Definition 15 and differs from the realized one by at most $\max\{1, \operatorname{Lip}(S)\}\,\varepsilon$ in the sup norm by (S2), which preserves excitation for ε small enough, ε being ours to choose. The Gram matrix Γ_k of (13c) is therefore

invertible, and (13d) returns the exact row except its forward coupling. Under Assumption 7 this includes $\hat{A}_k = A_k$, which is (17).

Residual and forward coupling. With the entries just obtained and $\hat{V}_j = V_j$ for $j \le k$, definition (13e) and (45) give the identity

$$\phi_k(t) = W_{k,k+1} S\big(V_{k+1}(t)\big), \tag{48}$$

valid at every t at which (45) holds, and in particular on the windows of (S3), where $\phi_k = W_{k,k+1} e_i$. Since $\{e_1, \dots, e_{n_{k+1}}\}$ spans $\mathbb{R}^{n_{k+1}}$, Lemma 10 applies with the design $\mathcal{E} = \{(e_i, [t_i^k + T, t_i^k + \tau + T])\}_i$ and gives $\hat{W}_{k,k+1} = W_{k,k+1}$. Hence $\hat{\Theta}_k = \Theta_k$.

Descent. By (S1) at rank $k+1$, $V_{k+1}(t) \in \Omega_\omega^{n_{k+1}}$ for $t \ge T^{(k+1)}$. Then $\hat{W}_{k,k+1}^\dagger \phi_k = W_{k,k+1}^\dagger W_{k,k+1} S(V_{k+1}) = S(V_{k+1})$ by Assumption 3 and (48), so that (13g) returns $\hat{V}_{k+1} = S^\dagger(S(V_{k+1})) = V_{k+1}$ by (4). This is $\mathcal{H}_{k+1}$.

A. Realization

It remains to produce a schedule in the sense of Definition 15 and a control realizing it. Assume $\mathcal{H}_k$ and apply, in this order, the three steps (a)–(c):

(a) **Regression.** Lemma 17 to layer 1, whose state is measured, and Lemma 13 to each layer $j \in [\![2, k]\!]$, whose saturation $S(V_j) = \hat{W}_{j-1,j}^\dagger \phi_{j-1}$ is available by $\mathcal{H}_k$ and by (48) at rank $j-1$; the references are $\gamma_1^{(k)}, \dots, \gamma_k^{(k)}$ and the margin is ε. Layer $k+1$ is held at $S(V_{k+1}) = 0$ by Lemma 11 with $v = 0$. Layers $j > k+1$ require no action, since they do not enter $\dot{V}_k$ at all, and enter $\dot{V}_{k+1}$ only through $W_{k+1,k+2} S(V_{k+2})$, which is bounded by $\bar{W}\sqrt{n_{k+2}}$. After a transient this yields (S1) and (S2) on $[r_k, r_k']$.

(b) **Forward coupling.** Lemma 12 on layer $k+1$, cycling $S(V_{k+1})$ through $e_1, \dots, e_{n_{k+1}}$ with dwell time $\tau_{\mathrm{d}} = \tau + T$, the feedbacks of (a) still holding layers $1, \dots, k$ in the band. This yields (S3). The control of layer $k+1$ is the open-loop law (25) with A_{k+1}^0 and B_{k+1} known. Empty when $k = p$.

(c) **Descent.** Lemma 13 to layer $k+1$, with measured signal $\hat{W}_{k,k+1}^\dagger \phi_k$, which equals $S(V_{k+1})$ by (48), and disturbance bound

$$\bar{\phi} = \bar{W} \sum_{j=1}^{\min(k+2,p)} \sqrt{n_j} \; + \; \bar{h}; \tag{49}$$

the gain ν is chosen above the threshold $\nu^\star$ of that lemma, which, like the smallness condition (23), is computable from the known data. After a time this brings layer $k+1$ into $\Omega_\omega^{n_{k+1}}$ and keeps it there, which is (S1) at rank $k+1$. Omitted when $k = p$.

The feedbacks of (a) are never switched off. Layer j keeps the law of Lemma 17 or of Lemma 13 from $T^{(j)}$ onwards, only its reference $\gamma_j^{(k)}$ changing from one stage to the next. This is what makes (S1) an invariant of the whole protocol rather than a property of a single stage, and it is what the induction hypothesis (44) records.

Each stage begins with a guard interval of length T, during which no estimator integrates and the differentiator reconverges from the jump of its input; the schedule of Definition 15 places every window after it. Between two saturation windows the control of layer $k+1$ vanishes, and by Proposition 16 the state returns to within $2R_\infty(0)$ within a relaxation interval of length T_{rel} (35); one single steering amplitude therefore serves every window (Section V-B), and the bound on layer $k+1$ is uniform in the number of windows. Each of (a)–(c) uses only the known data (8) and the estimates produced by the earlier stages, so the resulting control and estimator form a protocol in the sense of Definition 2. Summing the durations of (a)–(c) over k gives the total time T^*, every term of which is explicit in the known data. □

APPENDIX B
PROOF OF THEOREM 5

The proof of Theorem 4 applies unchanged; the only difference is that the full regressor (13b) replaces the reduced one (14). On the regression window the row identity (46) holds with the unknown A_k included in the fitted row, and the reference regressor is persistently exciting by Definition 15; the rest of the induction is unchanged. □

REFERENCES

[1] F. Giri and E.-W. Bai, *Block-oriented Nonlinear System Identification*, ser. Lecture Notes in Control and Information Sciences. Berlin: Springer, 2010, vol. 404.

[2] T. L. Vincent, C. Novara, K. Hsu, and K. Poolla, "Input design for structured nonlinear system identification," *Automatica*, vol. 46, no. 6, pp. 990–998, 2010. [Online]. Available: https://doi.org/10.1016/j.automatica.2011.01.063

[3] M. Gevers, "Identification for control: From the early achievements to the revival of experiment design," *European Journal of Control*, vol. 11, no. 4–5, pp. 335–352, 2005.

[4] H. Hjalmarsson, "From experiment design to closed-loop control," *Automatica*, vol. 41, no. 3, pp. 393–438, 2005.

[5] A. S. Bazanella, M. Gevers, and L. Miškovic, "Closed-loop identification of mimo systems: a new look at identifiability and experiment design," *European Journal of Control*, vol. 16, no. 3, pp. 228–239, 2010. [Online]. Available: https://doi.org/10.1016/j.ejcon.2010.05.004

[6] H. R. Wilson and J. D. Cowan, "Excitatory and inhibitory interactions in localized populations of model neurons," *Biophysical Journal*, vol. 12, no. 1, pp. 1–24, 1972. [Online]. Available: https://www.cell.com/biophysj/fulltext/S0006-3495(72)86068-5

[7] A. Destexhe and T. J. Sejnowski, "The Wilson-Cowan model, 36 years later," *Biological Cybernetics*, vol. 101, no. 1, pp. 1–2, 2009.

[8] M. Breakspear, "Dynamic models of large-scale brain activity," *Nature neuroscience*, vol. 20, no. 3, pp. 340–352, 2017.

[9] A. Hartoyo, P. J. Cadusch, D. T. Liley, and D. G. Hicks, "Parameter estimation and identifiability in a neural population model for electro-cortical activity," *PLoS computational biology*, vol. 15, no. 5, p. e1006694, 2019.

[10] B. J. Cook, A. D. Peterson, W. Woldman, and J. R. Terry, "Neural field models: A mathematical overview and unifying framework," *Mathematical Neuroscience and Applications*, vol. 2, 2022.

[11] C. Bernard, "Brain's best kept secret: Degeneracy," *Eneuro*, vol. 10, no. 11, 2023.

[12] E. Sorrell, M. E. Rule, and T. O'Leary, "Brain–machine interfaces: Closed-loop control in an adaptive system," *Annual Review of Control, Robotics, and Autonomous Systems*, vol. 4, pp. 167–189, 2021.

[13] R. Moran, D. A. Pinotsis, and K. J. Friston, "Neural masses and fields in dynamic causal modeling," *Frontiers in Computational Neuroscience*, vol. 7, p. 57, 2013.

[14] H. Elliott and W. Wolovich, "Parameter adaptive identification and control," *IEEE Transactions on Automatic Control*, vol. 24, no. 4, pp. 592–599, 1979.

[15] T. B. Burghi and R. Sepulchre, "Adaptive observers for biophysical neuronal circuits," *IEEE Transactions on Automatic Control*, vol. 69, no. 8, pp. 5020–5033, 2023.

[16] L. Brivadis, A. Chaillet, and J. Auriol, "Online estimation of hilbert-schmidt operators and application to kernel reconstruction of neural fields," in *2022 IEEE 61st Conference on Decision and Control (CDC)*. IEEE, 2022, pp. 597–602.

[17] ——, "Adaptive observer and control of spatiotemporal delayed neural fields," *Systems & Control Letters*, vol. 186, p. 105777, 2024.

[18] H. Wilson and J. Cowan, "A mathematical theory of the functional dynamics of cortical and thalamic nervous tissue," *Kybernetik*, vol. 13, no. 2, pp. 55–80, 1973.

[19] S.-i. Amari, "Dynamics of pattern formation in lateral-inhibition type neural fields," *Biological cybernetics*, vol. 27, no. 2, pp. 77–87, 1977.

[20] R. Postoyan, M. S. Chong, D. Nešić, and L. Kuhlmann, "Parameter and state estimation for a class of neural mass models," in *51st IEEE Conference on Decision and Control (CDC)*. IEEE, 2012, pp. 2236–2241.

[21] B. H. Jansen and V. G. Rit, "Electroencephalogram and visual evoked potential generation in a mathematical model of coupled cortical columns," *Biological Cybernetics*, vol. 73, no. 4, pp. 357–366, 1995. [Online]. Available: https://link.springer.com/article/10.1007/BF00199471

[22] G. Kreisselmeier and G. Rietze-Augst, "Richness and excitation on an interval—with application to continuous-time adaptive control," *IEEE Transactions on Automatic Control*, vol. 35, no. 2, pp. 165–171, 1990.

[23] S. Aranovskiy, A. Bobtsov, R. Ortega, and A. Pyrkin, "Performance enhancement of parameter estimators via dynamic regressor extension and mixing procedure," *IEEE Transactions on Automatic Control*, vol. 62, no. 7, pp. 3546–3550, 2017.

[24] G. Chowdhary and E. Johnson, "Concurrent learning for convergence in adaptive control without persistency of excitation," in *49th IEEE Conference on Decision and Control (CDC)*. IEEE, 2010, pp. 3674–3679.

[25] R. Ortega, S. Aranovskiy, A. A. Pyrkin, A. Astolfi, and A. A. Bobtsov, "New results on parameter estimation via dynamic regressor extension and mixing: Continuous and discrete-time cases," *IEEE Transactions on Automatic Control*, vol. 66, no. 5, pp. 2265–2272, 2020.

[26] A. M. Annabi, J.-B. Pomet, D. Prandi, and L. Sacchelli, "Identification of saturated networked systems," in *2025 IEEE 64th Conference on Decision and Control (CDC)*. IEEE, 2025, pp. 4208–4213.

[27] H. Weyl, "Über die gleichverteilung von zahlen mod. eins," *Mathematische Annalen*, vol. 77, no. 3, pp. 313–352, 1916.

[28] A. Levant, "Higher-order sliding modes and arbitrary-order exact robust differentiation," in *Proceedings of the European Control Conference*, 2001, pp. 996–1001.

[29] P. Bernard, L. Praly, and V. Andrieu, "Observers for a non-lipschitz triangular form," *Automatica*, vol. 82, pp. 301–313, 2017.

[30] A. F. Filippov, *Differential Equations with Discontinuous Righthand Sides*, ser. Mathematics and Its Applications. Kluwer Academic Publishers, 1988.